PACS 53.50.Td, 71.76, 72.80.Ey, 85.30.De, 85.30.Fg

A novel $Al_{0.33}Ga_{0.67}As/In_{0.15}Ga_{0.85}As/GaAs$ quantum well Hall device grown on (111) GaAs

H. Sghaier, L. Bouzaiene, L. Sfaxi, H. Maaref
Laboratoire de Micro-Optoélectronique et nanostructures de Monastir Faculté des Sciences de Monastir, Avenue de l'Environnement, 5000 Monastir (Tunisia)
Institut Supérieur d'Informatique et de Mathématiques de Monastir, Avenue de la corniche, Monastir

Abstract. In this study, we look at the advantages of (111) GaAs substrate over (001) one, when used to grow Hall devices by MBE. In top of that, we explore the consequence of a modified design of modulation doping pseudomorphic AlGaAs/InGaAs/GaAs, and we suggest a new quantum well structure for a Hall device grown on (111) GaAs substrate, with the objective of improving its performances. From self-consistent calculations, we find that the electron concentration n_s in the interface region is enhanced. This implies that one can have a wider spacer layer and still have the same n_s with the result that the mobility is improved. This result should be valuable for many types of devices. We specifically consider Hall sensors, where it is desirable to have a low electron concentration and high mobility.

Keywords: quantum well, Hall device, electron concentration.

Manuscript received 19.01.11; revised version received 29.12.11; accepted for publication 26.01.12; published online 29.03.12.

1. Introduction

Semiconductor magnetic field sensors such as Hall devices are widely used in many industrial and domestic applications. In recent years, Hall sensors using modulation-doped AlGaAs/InGaAs have been proposed [1-3]. Hall devices based on pseudomorphic heterostructures have attracted increasing interest recently by virtue of their high electron mobility combined with moderate sheet carrier densities, low temperature dependence of the output Hall voltage and large signal-to-noise ratios [4]. The AlGaAs/InGaAs system deserves special attention in this respect. It is the system of choice in the design of high-speed devices and RF circuits. Modulation-doped hetero-structures with a high electron mobility and low electron concentration can be used to achieve very high magnetic sensitivities [5].

Hall effect devices are by far the most widely used magnetic sensors today. Their future mainly depends on whether means will be developed to enhance their sensitivity and their temperature stability [6]. The key parameters for such devices which determine their sensitivity to magnetic field are their high electron mobility and low electron density. In a previous study, we have investigated the effect of piezoelectric field built in AlGaAs/InGaAs/GaAs pseudomorphic HEMT grown on (111)A substrate, and we have found that both electron density and mobility are enhanced [7]. In this paper, we combine results determined both in [6] and [7], and we report the design of a new two-dimensional electron gas Hall device based on AlGaAs/InGaAs/GaAs heterostructure, which was particularly optimized for low magnetic field measurements. Charge density profiles, total 2D electron densities, and sensitivities are calculated from coupled Schrödinger and Poisson equations. The main idea is to substitute a (111)A GaAs substrate to (001) one and to increase the mobility without decreasing the carrier concentration by means of special doping profile. Instead of having a δ-doped layer in a homogenous $Al_xGa_{1-x}As$ barrier material, we consider the possibility to have the donors in a narrow quantum well embedded in the barrier with a lower aluminum concentration than the rest of the barrier.

© 2012, V. Lashkaryov Institute of Semiconductor Physics, National Academy of Sciences of Ukraine

2. Device structure

The structure under investigation is presented in Fig. 1. It consists of Si-δ-doped $Al_{0.33}Ga_{0.67}As$ layer, an $In_yGa_{1-y}As$ thin layer and a p-type GaAs buffer layer. The Si δ-doped layer with a Si sheet concentration $2\cdot10^{12}cm^{-2}$ is separated from the QW by a variable thickness spacer layer. The conduction electrons are located in the 2D channel formed by the $In_yGa_{1-y}As$ layer with In composition y = 0.15 and thickness close to 10 nm. The role of the undoped spacer layer is to confine the electrons in the channel and to increase their mobility by separating the ionized donor atoms from the channel. The value of 10 nm of the channel width is dictated by the optimal In composition y = 0.15 from the viewpoint of of the crystal structure quality. Larger thicknesses in strained structures with the same In composition may give rise to lattice defects. In addition, a monolayer of InAs is inserted within the $In_yGa_{1-y}As$ channel to enhance the electron density in the active layer.

3. Theoretical considerations

Our calculations are based on a self-consistent solution of the one-dimensional Schrödinger and Poisson equations, in the effective mass approximation. The quantized energy levels E_i and their corresponding wave functions ψ_i, and the conduction band profile satisfy the following Schrödinger equation:

$$\left[-\frac{\hbar^2}{2}\frac{d}{dz}\left(\frac{1}{m^*(z)}\frac{d}{dz}\right)+U(z)\right]\Psi_i(z)=E_i\Psi_i(z). \qquad (1)$$

Where $m^*(z)$ is the position-dependant effective mass of the electrons and z is the growth direction. The potential $U(z) = U_C(z) + U_H(z) + U_{XC}(z) + U_{PZ}(z)$ is the sum of the conduction-band discontinuity $U_C(z)$ at the heterojunction, the Hartree potential energy $U_H(z)$, the exchange-correlation potential $U_{XC}(z)$ and the piezo-electric potential $U_{PZ}(z)$.

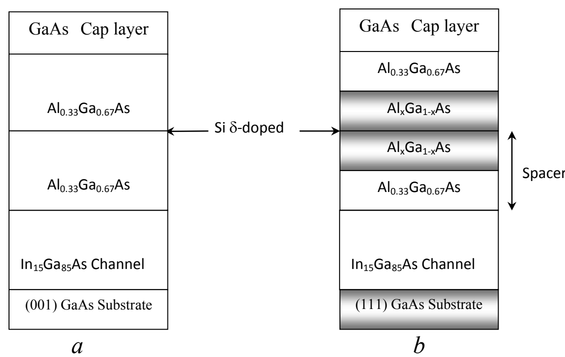

Fig. 1. a) Schematic cross-section of a conventional AlGaAs/InGaAs Hall heterostructure grown on (001) GaAs substrate. b) The same of the novel AlGaAs/InGaAs Hall heterostructure grown on (111) GaAs substrate.

The electrostatic potential energy is determined by the Poisson equation

$$\frac{d}{dz}\left[\varepsilon(z)\frac{d}{dz}U_H(z)\right]=\frac{e^2}{\varepsilon_0}\left[N_d(z)-N_a(z)-n(z)\right], \qquad (2)$$

where ε_0 is the electric constant of vacuum, ε is the dielectric permittivity of material, $N_d(z)$ is the three-dimensional density of the ionized donors, N_a is the residual acceptor concentration in the unintentionally doped GaAs, and $n(z)$ is the local density of the confined electrons,

$$n(z) = \sum_i n_i\left|\Psi_i(z)\right|^2 . \qquad (3)$$

At low temperatures, n_i can be written as:

$$n_i = \frac{m^*}{\pi\hbar^2}\left(E_F - E_i\right), \qquad (4)$$

where n_i is the carrier population in the ith subband, and E_F is the Fermi level. In the steady-state situation and at low temperatures, E_F is a constant and assumed to be pinned at the DX centre energy E_{DX} [8].

Therefore, the total sheet electron density in the channel, n_s, is the sum of the carrier population in all subbands, and can be written as follows:

$$n_s = \sum_i n_i . \qquad (5)$$

The exchange-correlation potential was approximated by the formula [9]

$$U_{XC}(z) = -0.916\frac{e^2}{6\pi\varepsilon_0\varepsilon_r}\left[\frac{3n(z)}{4\pi}\right]^{1/3} \qquad (6)$$

The piezoelectric potential may be written as:

$U_{PZ}(z) = eFz$.

Here, F is the magnitude of the piezoelectric field in the strained InGaAs layer, and it is given by the equation [10]:

$$F = \frac{2\sqrt{3}\,e_{14}\left(c_{11}+2c_{12}\right)}{\varepsilon_r\varepsilon_0\left(c_{11}+2c_{12}+4c_{44}\right)}\delta$$

where δ is the lattice mismatch, e_{14} is the piezoelectric coefficient, c_{11}, c_{12} and c_{44} are the elastic stiffness tensor coefficient.

In addition, we have taken into account the strain effects to evaluate the total potential energy. The following equations [11] have been used:

$E_c = A_c\,(e_{11} + e_{22} + e_{33})$, $A_c = -8.8 + 1.05y + 0.45y^2$,

where A_c is the deformation potential, y is the In concentration in the QW, and e_{ii} are the strain-tensor elements.

For the high-symmetric (001) growth direction, the strain elements are as follow [12]:

$$e_{11} = e_{22} = \delta,\quad e_{33} = \frac{-2C_{12}}{C_{11}}\delta .$$

© 2012, V. Lashkaryov Institute of Semiconductor Physics, National Academy of Sciences of Ukraine

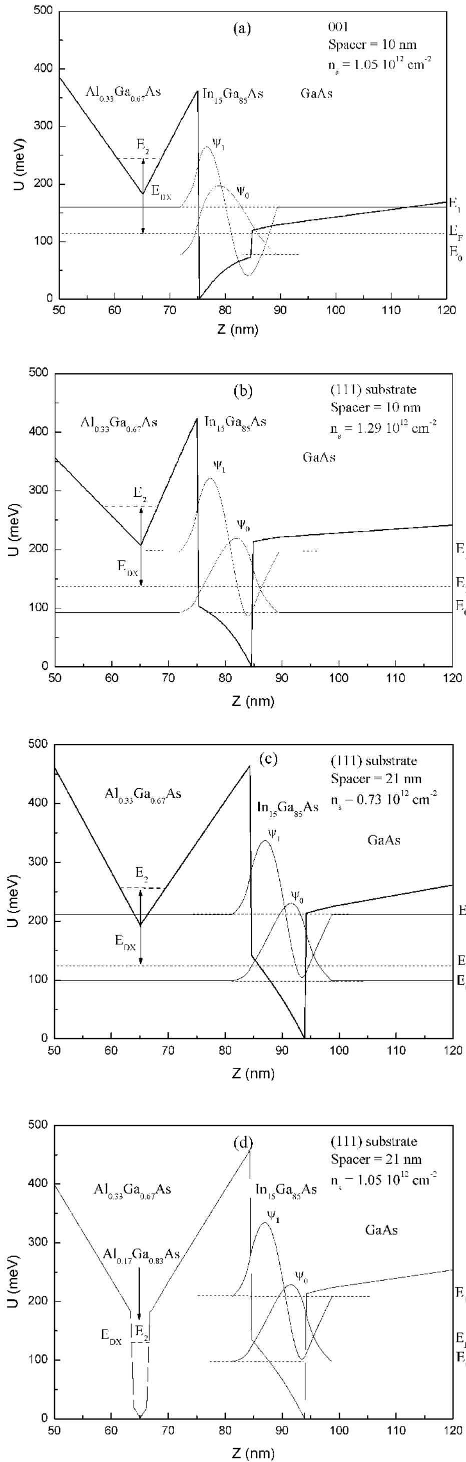

Fig. 2. Calculated band diagram for Hall structures: (a) conventional structure grown on (001) substrate with the spacer width 10 nm; (b) transitional structure grown on (111) substrate with the spacer width 10 nm; (c) transitional structure with the spacer width 21 nm; (d) novel structure (silicon in a quantum well) with the spacer width 21 nm, and the aluminum mole fraction 0.17. The lowest two subbands E_0 and E_1 are indicated together with the corresponding wave functions. E_2 represents the calculated energy of the lowest bound state localized to the embedded $Al_{0.15}Ga_{0.85}As$ layer. E_{DX} represents the DX center energy. The Fermi level is represented by the dashed line.

For high-symmetric (111) growth direction, the strain elements are as follow [12]:

$$e_{11} = e_{22} = e_{33} = \frac{4c_{44}}{c_{11} + 2c_{12} + 4c_{44}} \delta$$

with the lattice mismatch $\delta = (a_{GaAs} - a_{InGaAs})/a_{InGaAs}$.

The algorithm solves the one-dimensional Schrödinger equation along a series of slices in the growth direction. Each slice corresponds to one monolayer. After the Schrödinger's equation solution is taken, the carrier concentration calculated from Schrödinger's equation is substituted into the charge part of the Poisson's equation. The potential derived from the solution of Poisson's equation is substituted back to Schrödinger's equation. This solution process is continued until convergence is reached, and a self-consistent solution of Schrödinger's and Poisson's equation is obtained.

4. Results and discussions

The Hall voltage is given by

$$U_H = \alpha \frac{IB}{en_s}, \qquad (7)$$

where I is the current, B – perpendicular magnetic field, e – the electronic charge, n_s – sheet electron concentration, and α – geometric correction factor.

For a greek-cross structures where the length of active area is about one-third of the distance between contacts, $\alpha \approx 1$ [13]. Thus,

$$U_H \approx \mu EWB, \qquad (8)$$

where μ is the electron mobility, E – electric field in the active region of the Hall device, and W – width of the active region.

The latter relationship shows that the absolute sensitivity of the Hall device

$$S_A = \frac{dU_H}{dB} \approx \mu EW . \qquad (9)$$

Therefore, for high sensitivity devices, μ must be as high as possible.

On the other hand, the ratio of the absolute sensitivity to current is the current-related sensitivity,

$$S_I = \frac{1}{I}\frac{dU_H}{dB} \approx \frac{1}{n_s e}. \qquad (10)$$

The smaller n_s is, the higher S_I is. Thus, for high sensitivity devices, n_s must be as low as possible. However, this will lead to very high resistance devices, which will have a negative impact on noise performance.

In modulation-doped structures a two-dimensional electron gas is formed at the AlGaAs/InGaAs heterointerface due to the electron affinity difference between two materials. The electrons are separated from

© 2012, V. Lashkaryov Institute of Semiconductor Physics, National Academy of Sciences of Ukraine

Table. Electron density in the channel calculated for different aluminum mole fractions in the embedded QW in the barrier and for different spacer widths. The sample (a) represents the standard heterostructure grown on (001) substrate. The sample (d) grown on (111) substrate exhibits the same n_s as the sample (a), but has a larger spacer width, leading to much higher device sensitivity without degradation in noise characteristics.

Sample	a	b	c	d
Substrate orientation	(001)	(111)	(111)	(111)
Spacer thickness (nm)	10.0	10.0	21	21
Al mole fraction in the embedded QW	0.33	0.33	0.33	0.17
n_s (10^{12} cm^{-2})	1.05	1.29	0.73	1.05

the donors in the AlGaAs by a thin spacer layer, which decreases the impurity scattering, and enhances the electron mobility [14]. In theory, a higher value of the electron mobility can be obtained by increasing the spacer layer thickness. The spacer layer thickness controls the amount of charge trapped in the quantum well (QW), n_s and hence the current-related sensitivity (S_I). However, the cost of such improvement is a drastic loss of electron concentration in the channel, leading to a very high resistive device.

In a previous studies [15], we have shown that the charge density may be enhanced by introducing Si δ-doping in a thin $Al_xGa_{1-x}As$ QW embedded in the $Al_{0.33}Ga_{0.67}As$ barrier with x smaller than 0.33. We have observed an enhancement of the electron density when the aluminum concentration decreases. Thus, in order to compensate the charge density decrease in the channel due to spacer width increase, we suggest to realize δ-doping in a narrow QW within the $Al_{0.33}Ga_{0.67}As$ barrier where the Al concentration in the QW, must be as low as possible.

The goal of introducing δSi to narrow quantum well embedded in the barrier where the Al concentration is smaller than the Al concentration in the barrier is to compensate the DX centre effect in the common selectively doped $Al_xGa_{1-x}As$/InGaAs heterojunctions. The main idea was introduced by Schubert et al. [16]. The calculated results showed an enhancement of the 2DEG concentration at the heterointerface. We explain this electron concentration increase by the reduction of the DX centre energy with the decrease of aluminum in the $Al_xGa_{1-x}As$ layer, since the silicon atom is surrounded by three nearest group III atoms to which it is particularly related. In GaAs there is only one possible configuration around the DX site, and only one peak should be resolved in the DLTS signal, as confirmed by experiment [17]. In AlGaAs material, the group III atoms around the DX site can be any combination of Ga and Al. There are four possible configurations of these three nearest aluminum and/or gallium neighbors around each DX site [18]. According to these configurations, when the Al atomic environment of the silicon decreases, the DX centre energy decrease, too.

The spacer layer thickness and Al mole fraction in the embedded QW were used as variable parameters. The following four sets of parameters were considered:

a. The position of the inserted Si δ-doping with reference to the left side of the QW was selected to be 10 nm. The aluminum mole fraction x = 0.33, substrate (001) GaAs.
b. The position of the inserted Si δ-doping with reference to the left side of the QW was selected to be 10 nm. The aluminum mole fraction x = 0.33, substrate (111)A GaAs.
c. The position of the inserted Si δ-doping with reference to the left side of the QW was selected to be 21 nm. The aluminum mole fraction x = 0.33, substrate (111)A GaAs.
d. The position of the inserted Si δ-doping with reference to the left side of the QW was selected to be 21 nm. The aluminum mole fraction x = 0.17, substrate (111)A GaAs.

The calculated results are shown in Fig. 2, which correspond to the above four sets (a), (b) (c) and (d), respectively. Each figure displays the self-consistent conduction-band potential profile and the first two energy levels as well as the corresponding wave functions. In Table, we have reported the calculated electron density in the channel for the same samples.

The sample (a) represents a conventional AlGaAs/InGaAs-based magnetic sensor, grown on (001) GaAs substrate, and it is being used as reference in this study.

The sample (b) is similar to the sample (a), but grown on (111)A GaAs substrate. We notice two important things. First, an enhancement of the electron density which is mainly due to the incorporation of a piezoelectric field within the pseudomorphically strained active layer in the structure grown on (111) GaAs substrate [7]. Second, a shift of the waveform ψ_0 to the right side by almost 5 nm. The latter displacement should improve the special separation between confined electrons and ionized dopants, leading to increased electron mobility.

The sample (c) with a larger spacer thickness exhibits the lower electron density. When the spacer is increased, the electron mobility μ increases too, as the latter is approximately proportional to the third degree of the spacer width [14]. Thus, the sample (c) features a better absolute magnetic sensitivity than the sample (b), since S_A is proportional to μ. However, we notice a drastic decrease of the electron density, leading to a very high resistance device, which has a negative impact on noise performance.

The sample (d) represents the proposed novel structure. Compared to the conventional structure, the novel structure shows larger spacer width and has the same electron concentration in the channel. Therefore,

© 2012, V. Lashkaryov Institute of Semiconductor Physics, National Academy of Sciences of Ukraine

S_A is enhanced, and S_I remains unchanged, since n_s is the same for both samples (a) and (d). The results reported in Table show that the absolute magnetic sensitivity may be enhanced by

$$\frac{\mu_d}{\mu_a} \approx \left(\frac{\text{spacer}_d}{\text{spacer}_a} \right)^3 > 9 , \qquad (11)$$

where μ_a and μ_d are, respectively, the mobility of sample (a) and sample (d), and spacer_a and spacer_d are, respectively, the spacer thickness of sample (a), and sample (d).

5. Conclusions

In this paper, we have described the design of a Hall sensor using AlGaAs/InGaAs/GaAs quantum well structure grown on (111)A GaAs substrate, with the goal of improving its sensitivity. Charge density profiles, total 2D electron densities, and sensitivities are calculated from coupled Schrödinger and Poisson equations. The main idea is to take advantage of the enhanced charge density provided by using (111) oriented GaAs substrate and to increase the mobility without decreasing the carrier concentration by means of special doping profile. The results are potentially useful and have a direct impact on the design of highly sensitive Hall devices based on AlGaAs/InGaAs heterostructures, since it has been demonstrated that the magnetic sensitivity of our proposed structure may be as higher as 9 times than that of existing pseudomorphic Hall sensors grown on (001) substrate.

References

1. V. Mosser, S. Abdoulhouda, J. Denis, S. Contreras, Ph. Lorenzini, F. Kobbi, J.L. Robert // *Sens. Actuators A*, **41-42**, p. 450-454 (1994).
2. V. Mosser, S. Contreras, S. Abdoulhouda *et al.* // *Sens. Actuators A*, **43**, p. 135-140 (1994).
3. N. Nahed, M. Missous // *Sens. Actuators A*, **102**, p. 216-222 (2003).
4. J.S. Lee, K.H. Ahn, Y.H. Jeong, D.M. Kim // *Sens. Actuators A*, **57**, p. 183-185 (1996).
5. V.P. Kunets *et al.* // *Sens. Actuators A*, **101**, p. 62-68 (2002).
6. H. Sghaier, L. Bouzaiene, L. Sfaxi, H. Maaref // *J. Appl. Phys*. **100**, 044316 (2006).
7. L. Bouzaiene, H. Sghaier, S. Rekaya, L. Sfaxi, H. Maaref // *Appl. Phys. A*, **80**, p. 295-299 (2005).
8. A. Leuther, A. Förster, H. Lüth, H. Holzbrecher, U. Breur // *Semicond. Sci. Technol.* **11**, p. 766-771 (1996).
9. P. Ruden and G.H. Dohler // *Phys. Rev. B*, **27**, p. 3538-3546 (1983).
10. T.S. Moise, L.J. Guido, J.C. Beggy, S. Seshari, T.J. Cunningham, R.C. Barker // *J. Electron. Mater.* **21**, p. 119 (1992).
11. C. Kopf, H. Kosina, S. Selberherr // *Solid State Electron*. **41**, p. 1139 (1997).
12. E.A. Caridi, J.B. Stark // *Appl. Phys. Lett.* **60**, p. 1441 (1992).
13. R.S. Popovic, *Hall Effect Devices*. Adam Hilger Publishing, Bristol, 1991, p. 165-170.
14. T. Ando, B. Fowler, F. Stern // *Rev. Mod. Phys.* **54**, p. 437 (1982).
15. L. Bouzaiene, L. Sfaxi, H. Sghaier *et al.* // *Opt. Mater*. **17**, p. 299-303 (2001).
16. E.F. Schubert, J.E. Cunningham, W.T. Tsang, G.L. Timp // *Appl. Phys. Lett.* **51**(15), p. 1170-1172 (1987).
17. P.M. Mooney, T.N. Theis, S.L. Wright // *J. Electron. Mater.* **20**, p. 23 (1991).
18. P.M. Mooney // *Semicond. Sci. Technol. B*, **1**, p. 6 (1991).

© 2012, V. Lashkaryov Institute of Semiconductor Physics, National Academy of Sciences of Ukraine